Chapter 3

Cu Contamination Removal with Metal Chelators

3.1 Introduction

Due to copper has low resistivity and high electromigration resistance, it has been used as the interconnect material in the semiconductor industry. However, several important issues remain to be overcome for Cu integration. After Cu CMP process, wafer surface leaves a large amount of copper contaminations on the surface. The ITRS road map [23] suggests for 90nm technologies that critical metals have to be reduced to below 10^{10} atom/cm^2. Figure.1-6 shows the Pourbaix diagram of Cu-H_2O system. It indicated that copper is corroded in acidic and alkaline solutions easily. Therefore, the metallic contamination on oxide surfaces can be due to both the adsorption of dissolved metal species and the precipitation of insoluble metal compounds on wafer surface. Copper deep levels in the silicon band gap can act as recombination centers, hence reducing minority carrier lifetime. The consequence could cause higher leakage current between adjacent interconnection lines. Therefore, the availability of a post-Cu CMP cleaning process that effectively removes contamination from all regions of the wafer (front, back, and edge), leaving a clean surface for the subsequent process steps, is critical to the adoption of copper technology.

In this study, various metal chelators, citric acid, and acetic acid, containing carboxyl acid group (-COOH) were investigated to reduce the copper contamination from ILD surface because metal chelator can react with metallic impurities to form stable metal-chelate complexes. The chemical structure of metal chelators is showed in Figure.3-1. We would compare with their cleaning efficiency and corrosion effect. Furthermore, the influences of cycle time, concentration and pH value were also studied.

3.2 Experimental Procedures

3.2.1 Wet Ability Test with Metal Chelators on Oxide Surface

A p-type (100) 6-inch-diameter silicon wafer was used as the substrate material in this study. A 2000A thick SiO_2 was deposited by plasma enhanced chemical vapor deposition (PECVD). The PECVD deposition was performed with STS multiplex cluster system. After depositing, the contact angle of metal chelators on oxide surface was measured to observe the wetting ability. The concentration of metal chelators was $5x10^{-4}$M, 10^{-3}M, $5x10^{-3}$M and 10^{-2}M and each drop was fixed at 3ul.

3.2.2 Corrosion Test with Metal Chelators on Copper Surface

The substrates used in these experiments were 6-inch-diameter p-type (100) oriented silicon wafers. First, a 2000A thick SiO_2 was deposited by PECVD. After depositing, 500A thick Ta barrier metal layer and 1000A thick Cu film was continuously deposited by sputtering. The sputter deposition was performed with ULVAC SBH-3308 RDE sputter system. The etching rate of the Cu wafer was evaluated by immersed in the metal chelators for 1 hour and measuring the change in sheet resistance at 9 points (Figure.3-2) on the Cu wafer before and after immersed. The concentration of metal chelators was $5x10^{-4}$M, 10^{-3}M, $5x10^{-3}$M and 10^{-2}M. The sheet resistance was measured by a four point probe (Napson RT-80/RG-80).

3.2.3 Electrochemical Measurement

In order to understand the corrosion reaction further, polarization curve scans of copper in the metal chelators being studied were carried out on an EG&G Potentionstat Model 273. The working electrode was 99.99% copper cylinder (0.05mm in thickness), with an area of $0.5cm^2$ exposed to the metal chelators. The reference and counter electrode were SCE (standard calomel electrode) and Pt, respectively. The polarization scans were recorded by scanning from negative voltage (0.25V below the open circuit potential) to positive voltage

with a voltage scan rate of 1mV/s and the disk holder speed was 300rpm.

3.2.4 Cleaning Efficiency with Metal Chelators

3.2.4.1 Sample Preparation

The experiment flow was shown in Figure.3-3. A p-type (100) 6-inch-diameter silicon wafer was used as the substrate material in this study. A 2000A thick SiO_2 was deposited by PECVD. The polishing process was performed in order to make the Cu ions bonded on the oxide layer uniformly before immersed in $CuSO_4$ solution. The polishing recipes and slurry formulations were listed in the Table.3-1. Then, the polished oxide wafer was immersed in the 1M $CuSO_4$ solution for 1 minute. After that, the polished oxide wafer was cleaned using de-ionized Water (D. I. Water) by the post-CMP cleaner of Solid State Equipment Corporation MODE 50 (SSEC-M50). The duration of cleaning was 7 cycles (15 cycles/min) and the rotation rate of wafer was 800 rpm. Then, the polished oxide wafer was dry spun at the rotation rate of 2500 rpm and the first TXRF analysis was performed to calculate the amount of Cu ions. Two types of metal chelators cleaning were performed on the SSEC-M50 cleaner. Table.3-2 listed the cleaning steps and parameters of SSEC-M50. Then, the second TXRF analysis was performed to determine the cleaning efficiency.

3.2.4.2 CMP and Post-CMP Cleaning Process

Polisher Setup

In this study, we use the CMP machine (Figure.3-4) which is IPEC/Westech Model 372M CMP processor. The CMP machine consists of a wafer carrier and a primary circular polishing table mounted with Rodel IC 1400^{TM} grooved (made of polyurethane impregnated polyester) pad and a secondary buffing table mounted with an Rodel Politex Regular E.^{TM} pad, a carrier to hold wafers against the pad, and a Rodel R200-T3 carrier film to provide buffer between the carrier and wafer was used for CMP process. Recesses in the carrier template

mechanically constrain a single 6-inch wafer, preventing it from sliding out from under the carrier during polishing. A polymeric film placed in the recess brings the wafer slightly above the surrounding template surface. When the film is wetted, it provides sufficient surface tension to hold the wafer while it is being positioned over the polishing table. The teflon retaining ring is recessed from the wafer surface about 7 miles. The slurry, pumped out from a reservoir at a controlled rate, is delivered to a point near the center of the table. The table and the carrier are both motor driven spindles, rotated independently at constant angular velocities (rpm). The arm is oscillated about their position at half radius of the table to utilize more pad area and to reduce pad wear [35]. Pressure at the wafer-slurry-pad interface is controlled via an overhead mechanism, which allows pressure to be applied onto the wafer carrier.

Post-CMP Cleaning

After the CMP process, the polished wafers were cleaned by the post-CMP cleaner of Solid State Equipment Corporation MODE 50 (SSEC-M50). The cleaning for residual contaminations was implemented by the PVA brush scrubbing with varied cleaning solutions. The PVA brush scrubbing technology has been employed for many years and considered to be the most effective method for removing particles. Each of the polished wafers must be processed by cleaner immediately after polishing to avoid slurry drying.

3.3 The Performances of Metal Chelators

Wetting Ability

When a drop of liquid is dropped onto the surface of a solid, the angle between the surface and the tangent line of the liquid droplet is called the contact angle. The contact angle tells how well a liquid wets a solid, the smaller the angle, the better the wetting ability. Young's equation describes the balance of forces at the liquid-vapor-solid three-phase line (Figure.3-5):

$$\gamma_{SV} - \gamma_{SL} = \gamma_{LV} \cos\theta \qquad \text{(Eq.3-1)}$$

where the interfacial tensions between solid and liquid (γ_{SL}), that between solid and vapor (γ_{SV}) and that between liquid and vapor (γ_{LV}) interface, and θ is the contact angle [36]. In this study, the wetting ability of the metal chelators was analyzed by the contact angle system (KRuSS GmbH). Good wetting ability would ensure the metal chelators coved whole wafer surface. Then, Metallic contamination removal was uniform.

Cu Film Thickness Measurement

In this study, thickness of the Cu film was calculated by dividing the film resistivity with its measured sheet resistance. The relation between thickness and resistivity was given by

$$\rho = R_s \cdot t \qquad \text{(Eq.3-2)}$$

where ρ was the resistivity (μΩ•cm/□), R_S was the sheet resistance (μΩ/□) and t was the Cu film thickness. We assume that the resistivity of the Cu film was not changed by the processing. The resistivity of Cu film in our experiment was in the range from 1.8 μΩ•cm/□ to 2.3 μΩ•cm/□.

The sheet resistance of the Cu film was measured by the four-point probe (Model RT-80/RG-80 mapping system). For a thin wafer with thickness t much smaller than either a or d, the sheet resistance R_s was given by

$$R_s = CF \cdot \frac{V}{I} \qquad \text{(Eq.3-3)}$$

where CF was the correction factor (Figure.3-6). In the limit when d»S, where S was the probe spacing, the correction factor becomes (π/ln 2)=4.54 [37].

The etch rate of blanket Cu films were calculated by following formula:

$$\text{Etch Rate} = \frac{\text{(Pre-etch thickness)- (Post-etch thickness)}}{\text{Etch time}} \qquad \text{(Eq.3-4)}$$

Electrochemical Analysis

In this study, the electrochemical system was EG&G Potentionstat Model 273. The electrochemical apparatus using three electrodes been shown in Figure.3-7. That been consists of a rotor where a working electrode was attached. The working electrode was made of a copper (99.99%) cylinder whose area was 0.5cm^2. A Pt mesh plate and a standard calomel electrode (SCE) were used as counter and reference electrodes. A potentiostat changed electrical current to the test electrode potential from its open circuit potential (OCP), to a potential value that was determined by the magnitude of potentiostat current. Test electrode polarization was measured as a potential difference between reference and test electrodes. No electrical current flowed between a potentiostat and reference electrodes, so it remained at its OCP and provided a fixed reference point for corrosion measurement. The reference electrode was also used provide feedback to the potentiostat, so that test electrode potential could be monitored and adjusted to a desired level [38].

TXRF Analysis

The total reflection X-ray fluorescence spectrometry (TXRF) could sensitively detect the metallic impurities on surface. In this study, TXRF was used to decide the amount of Cu ions. The Cu contamination on the dielectric surface was detected using an ATOMIKA 8030W TXRF system. TXRF was based on the photoelectric effect. When an atom irradiated with highly energetic photons, an electron from one of the inner shells might be ejected. As the vacant place was filled by an electron from an outer shell, a photon whose energy was characteristic of the atom was released. This radiation was called fluorescent radiation and detected by an energy dispersive detector. TXRF made use of total reflection of the primary X-ray beam at grazing incidence (Figure.3-8) [39][40]. The high reflectivity in the total reflection mode resulted in an extremely low energy transfer from the incident beam into the irradiated substrate, because most of the energy was reflected and does not penetrate through

the interface.

3.4 Results and Discussions

3.4.1 Wetting Ability

The wetting ability of metal chelators was investigated by contact angle measurement. Table.3.3 listed contact angle of metal chelators with various concentrations on oxide surface. All of contact angles were small. It indicated that two kinds of metal chelators were easier to moisten the oxide surface and better wetting ability. Hence, they could uniformly remove copper contamination.

3.4.2 Copper Corrosion

The results of corrosion test on copper surface with metal chelators for 1hour, as shown in Figure.3-9. As the concentration of metal chelators was increased, the etching rate for copper was increased. The etching rate for copper with acetic acid was higher than citric acid. However, the etching rate was low for copper with two kinds of metal chelators, even in high concentration.

3.4.3 pH Effect on Copper Corrosion

In this study, the pH of metal chelators was modified by KOH. The result of copper corrosion with metal chelators at various pH values, as shown in Figure.3-10 and Figure.3-12. This showed that the etching rate for copper with metal chelators in the alkaline environment was lower than in the acidic environment. According to the Pourbaix diagram, it indicated that Cu_2O formation is likely at low potentials. CuO forms on copper at higher potentials between pH=7 to pH=13. Because copper surface was oxidized to form copper oxide passivation, the etching rate was reduced in the alkaline environment. Figure.3-11 and Figure.3-13 showed the Tafel diagrams. It showed that corrosion current in the alkaline environment was lower than in

the acidic environment. Hence, it also indicated that copper surface was oxidized to form copper oxide passivation in the alkaline environment.

3.4.4 Cleaning Efficiency

In this study, the initial Cu contamination level was controlled at the range of about $100x10^{10}$ to $200x10^{10}$ atoms/cm^2 before cleaning process. Figure.3-14 showed the results of cleaning efficiency with various cleaning cycles. As cleaning cycle was increased, the residual copper contamination was decreased. The cleaning efficiency of citric acid would be saturated after 40 cycles (15 cycles/min), and copper contamination concentration was below the detection limit of TXRF. In compared with citric acid, the cleaning efficiency of acetic acid was obviously worse. Hence, wafer surface still left a large amount of copper contaminations. This is duo to citric acid had three carboxyl groups and one hydroxide group that could coordinate with Cu ions. Contrarily, acetic acid had only one carboxyl group and exhibited the worse cleaning efficiency. Figure.3-15 showed the results of cleaning efficiency with various concentrations. As the concentration of citric acid was increased, the efficiency of copper contamination removal almost did not change and copper contamination concentration was below the detection limit of TXRF. It indicated that citric acid with low concentration had enough ability to remove the most Cu ions. However, acetic acid with high concentration still left a large amount of copper contaminations on oxide surface.

3.4.5 pH Effect on Cleaning Efficiency

The pH of cleaning solutions would influence chelating capability owing to the varying activing of protonated or deprotonated functional groups. For a metal chelator, Y, the chelating reaction for a metal ion M could be represented as [41]:

$$M + Y \leftrightarrow MY$$

$$\beta \; H^+$$

$$HY, H_2Y, H_3Y, ... \quad \text{(Eq.3-5)}$$

when the Eq.3-5 reached equilibrium state, the total concentration of Y which did not complex with metal ions was given by:

$$c_Y = [Y] + [HY] + [H_2Y] + [H_3Y] + ... \quad \text{(Eq.3-6)}$$

The concentration of Y in the solution was given by:

$$\alpha_Y = \frac{[Y]}{[c_Y]}$$

$$= \frac{[Y]}{[Y] + [HY] + [H_2Y] + [H_3Y] + ...}$$

$$= \frac{1}{1 + \frac{[HY]}{[Y]} + \frac{[H_2Y]}{[Y]} + \frac{[H_3Y]}{[Y]} + ...} \quad \text{(Eq.3-7)}$$

The proton equilibrium-constant was given by

$$\beta_n = \frac{[H_nY]}{[Y][H^+]^n} \quad \text{(Eq.3-8)}$$

$$\frac{[H_nY]}{[Y]} = \beta_n[H^+] \quad \text{(Eq.3-9)}$$

Substituting Eq.3-9 into Eq.3-7, the expression of α_Y could now be written as:

$$\alpha_{Y(H)} = \frac{1}{1 + \sum_{i=1}^{n} \beta_i [H^+]^i} \quad \text{(Eq.3-10)}$$

A high value of α_Y was always desirable for achieving good chelating capability. This was achieved, according to Eq.3-10, at a high pH of cleaning solutions.

Figure.3-16 and Figure.3-17 showed the results of cleaning efficiency of citric acid with various cleaning cycles and various concentrations. The results showed clearly that citric acid in the acidic environment had better cleaning efficiency than in the alkaline environment. The result of acetic acid was similar, as shown in Figure.3-18 and Figure.3-19. Copper was oxidized to copper oxide in the alkaline environment. Because metal chelators could not chelate with copper oxide, the cleaning efficiency reduce in the alkaline environment.

3.5 Summary

In this study, we studied the cleaning efficiency and corrosion effect of metal chelators. Citric acid and acetic acid have low contact angle and corrosion rate, so they could remove uniformly copper contamination without causing corrosion to the damascene copper interconnects.

In addition, citric acid has three carboxyl groups and one hydroxide group that could coordinate with Cu ions. Hence, citric acid has the better cleaning efficiency than acetic acid, and that citric acid with low concentration had enough ability to remove the most Cu ions has been investigated. Furthermore, copper was oxidized to copper oxide in the alkaline environment. Metal chelators could not chelate with copper oxide, and cleaning efficiency would reduce in the alkaline environment.

Table.3-1 Polishing parameters for cleaning experiment.

IPEC 372M	***Phase1***	***Phase2***
Down force	5.0 psi	2.0 psi
Back pressure	1.5 psi	0 psi
Platen/carrier speed	42/45 rpm	20/25 rpm
Slurry flow rate	150 ml/min	150 ml/min
Polishing Time	60 sec	20 sec
Polishing Pad	Rodel Politex Regular E.™	
Carrier Film	Rodel R200 T3	
Slurry formulation	30wt.% SS-25	DIW rinse

Table.3-2 The cleaning steps and parameters of SSEC-M50.

SSEC-M50		***Cleaning time***	***Flow rate***	***Rotation rate of water***
Step1	***Chelator cleaning***	Parameter (15 cycles/min)	150 ml/min	800 rpm
Step2	***DIW rinse***	7 cycle (15 cycles/min)	unknown	800 rpm
Step3	***Dry spin***	25 sec	off	2500 rpm

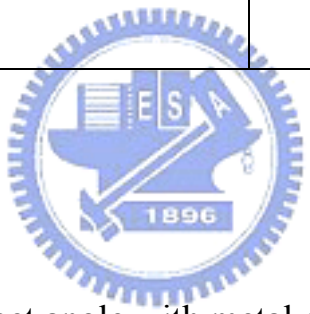

Table.3-3 Result of contact angle with metal chelators

Chelator concentration	***Contact angle of citric acid***	***Contact angle of acetic acid***
$4E^{-4}M$	16.7°	18.2°
$1E^{-3}M$	18.9°	17.9°
$5E^{-3}M$	16.4°	17.1°
$1E^{-2}M$	17.7°	19.1°

Citric acid

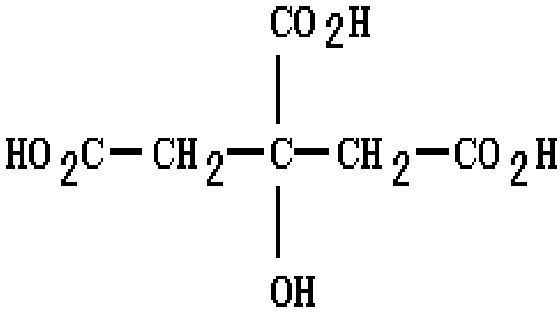

Acetic acid

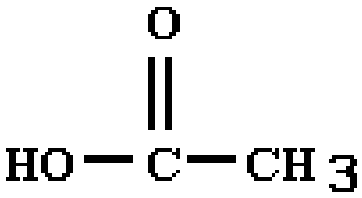

Figure.3-1 Metal chelators used in this study

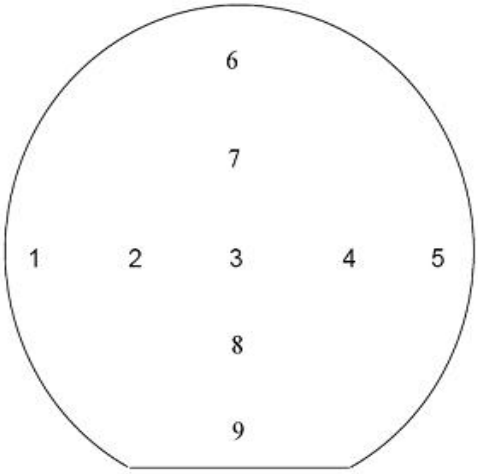

Figure.3-2 Contact angle measuring points in the wafer surface

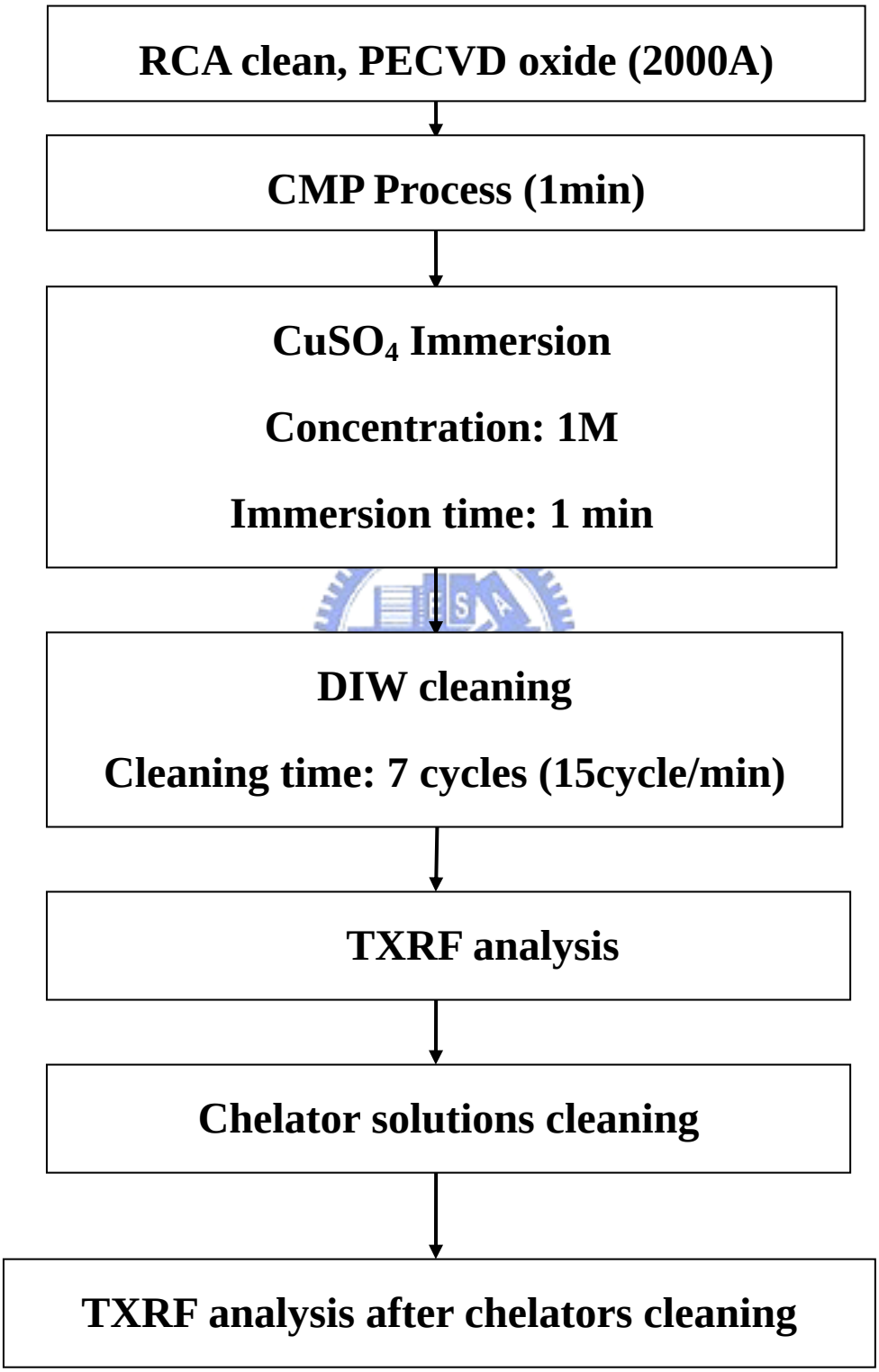

Figure.3-3 The cleaning experiment flow

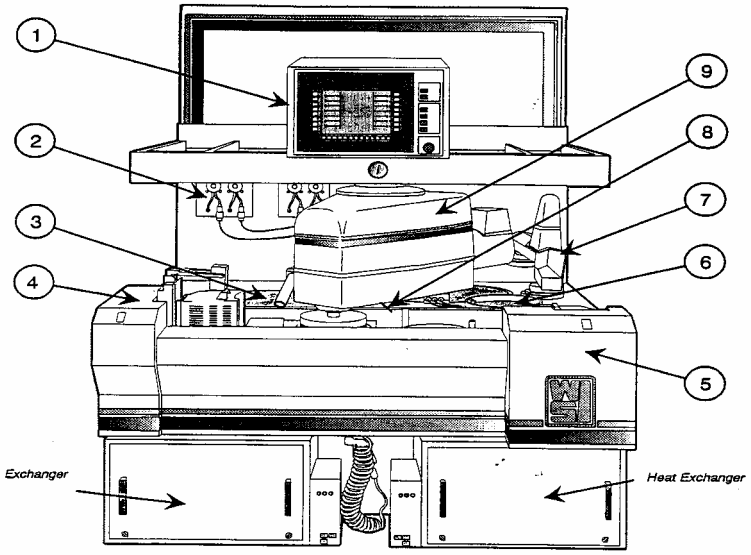

1 - Control Console & Overarm
2 - Slurry Motors & Slurry Final
3 - Platens and Drains
4 - Unload Station
5 - Load Station
6 - Clean Station & Slurry Primary
7 - Rotating Pad Conditioner II
8 - Polish Arm Drive
9 - Polish Arm
- Heat Exchanger

(a)

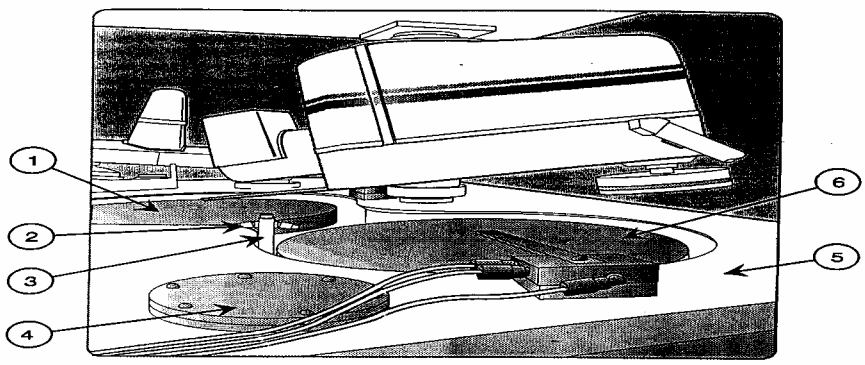

1 - Primary Platen, Cooled (372-21110)
2 - Spray Nozzle (372M-44160)
3 - Spray Tube (372M-44160)
4 - Pad Conditioner Cover (372M-44160)
5 - Contour Top (372M-44160)
6 - Final Platen, Cooled (372-21111)

(b)

Figure.3-4 (a) Schematic diagram of the Westech Model 327M CMP polisher
(b) Platen assemblies of the Westech Model 327M CMP polisher.

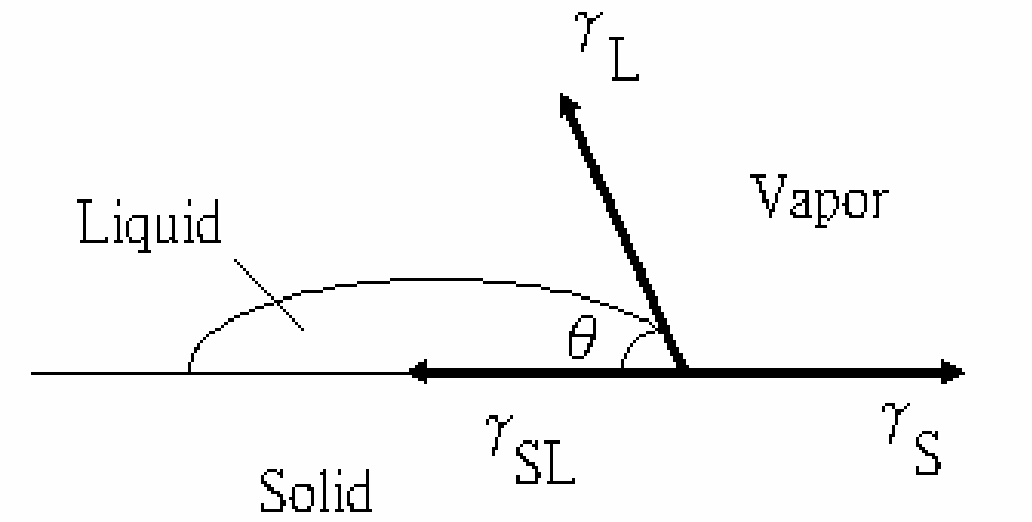

Figure.3-5 Diagram of a liquid drop showing the contact angle.

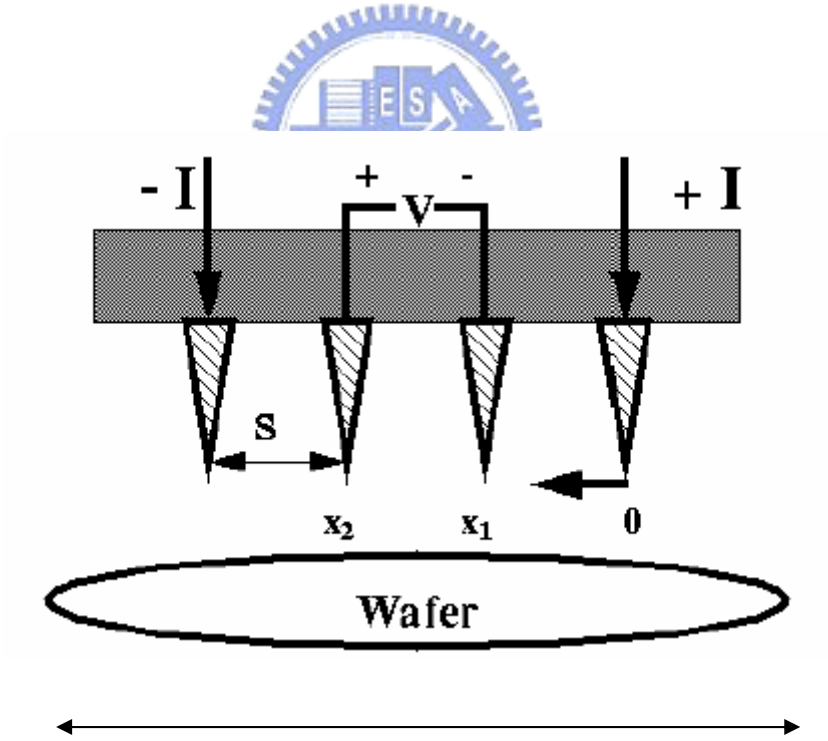

Figure.3-6 Schematic of 4-point probe configuration.

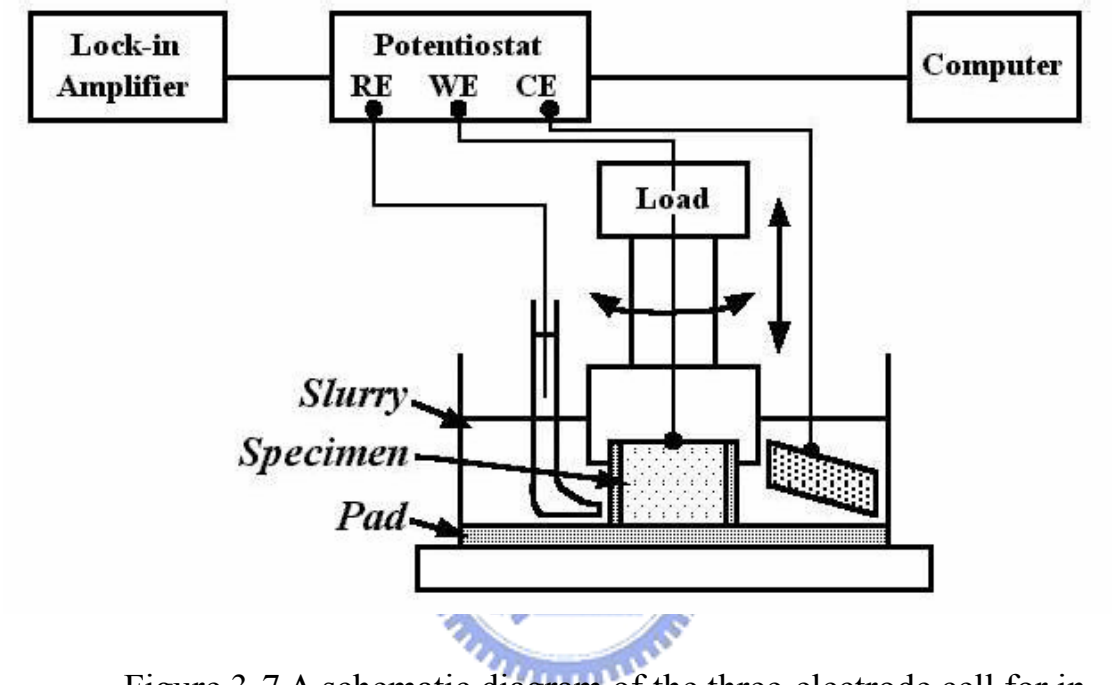

Figure.3-7 A schematic diagram of the three-electrode cell for in situ electrochemical measurements

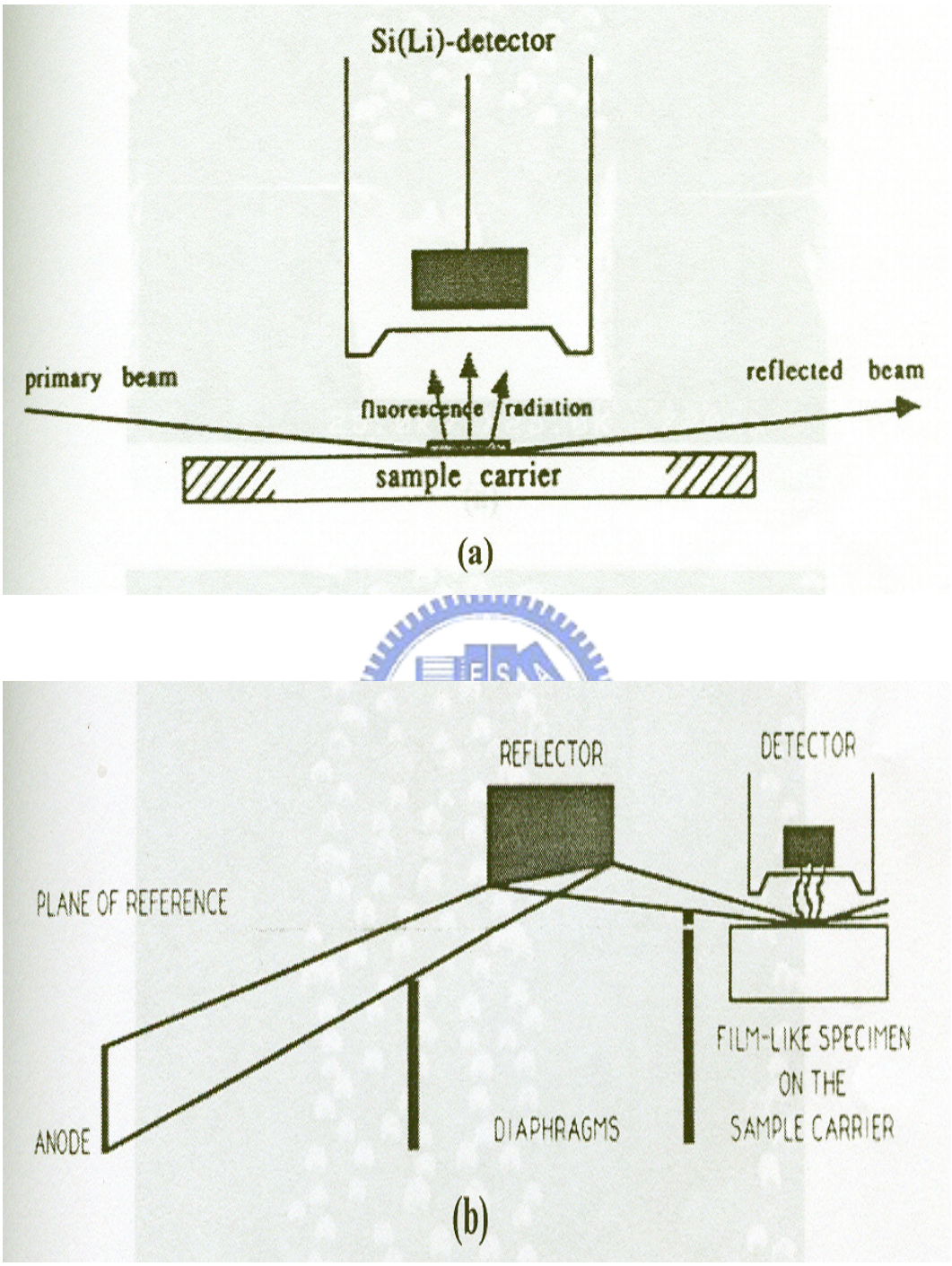

Figure.3-8 (a) Arrangement for TXRF analysis
(b) Path of the X-rays in a commercially available TXRF instrument

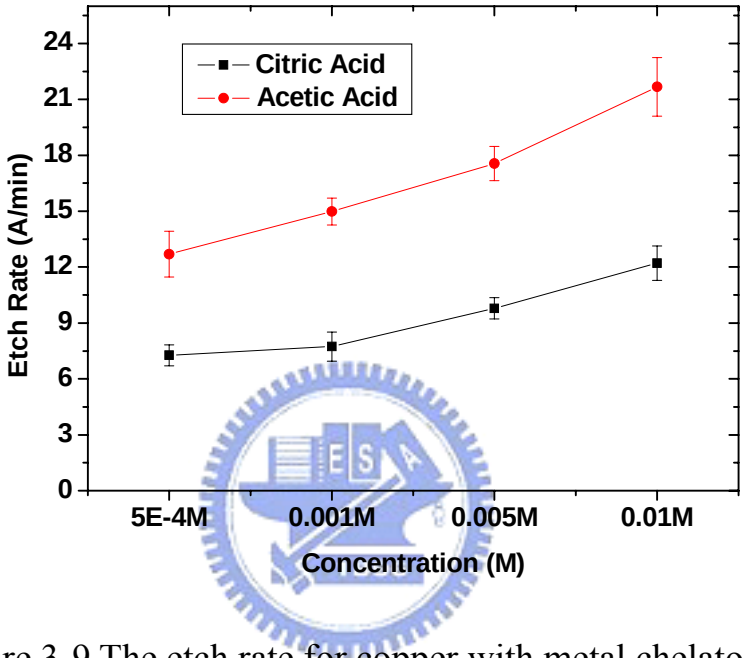

Figure.3-9 The etch rate for copper with metal chelators.

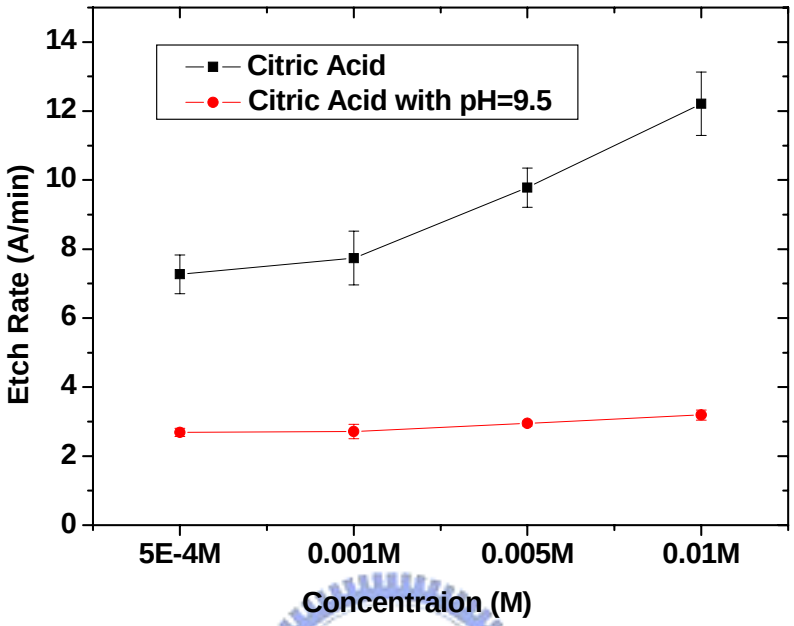

Figure.3-10 The etch rate as a function of citric acid concentration with different pH.

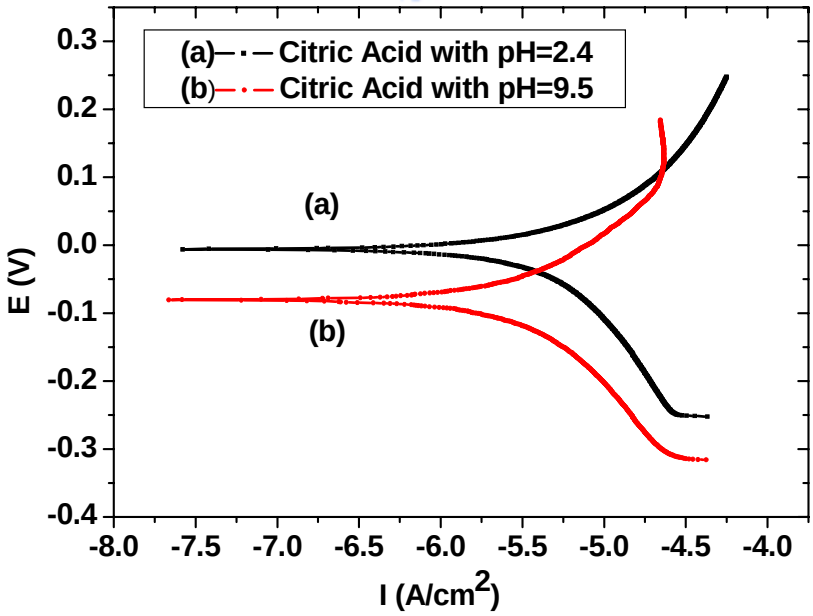

Figure.3-11 Tafel diagram of acetic acid with different pH

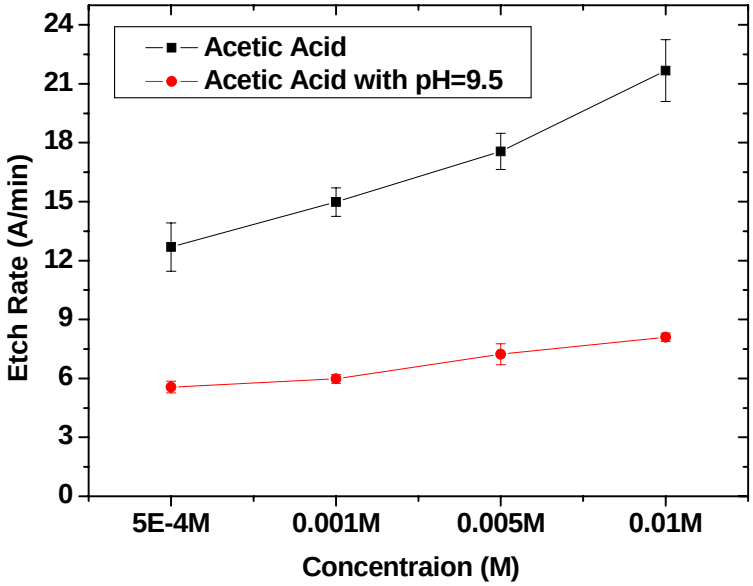

Figure.3-12 The etch rate as a function of acetic acid concentration with different pH.

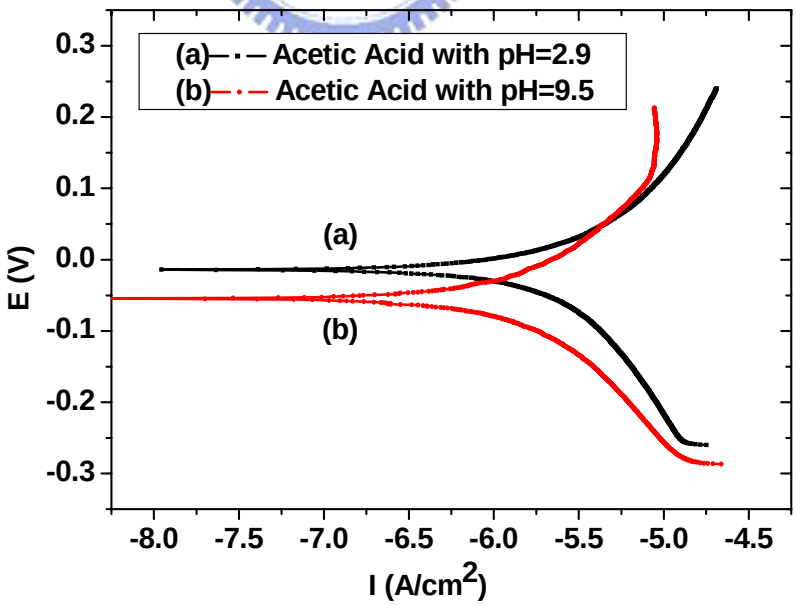

Figure.3-13 Tafel diagram of acetic acid with different pH

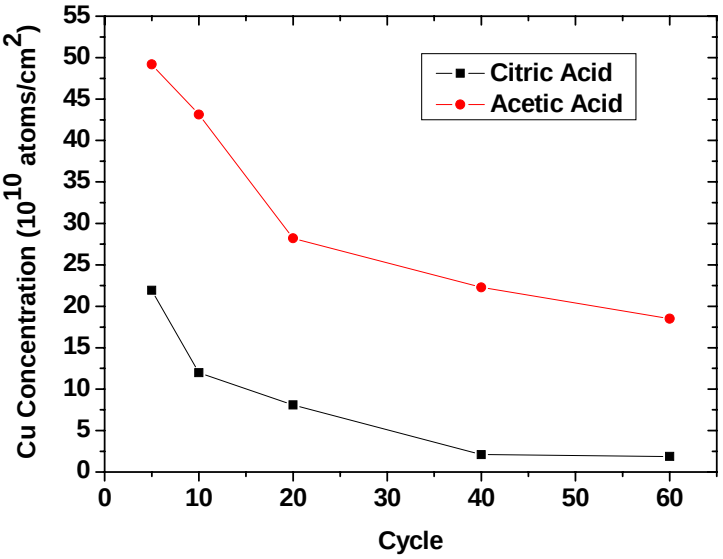

Figure.3-14 The cleaning efficiency as a function of cycle with concentration=5E^{-4}M.

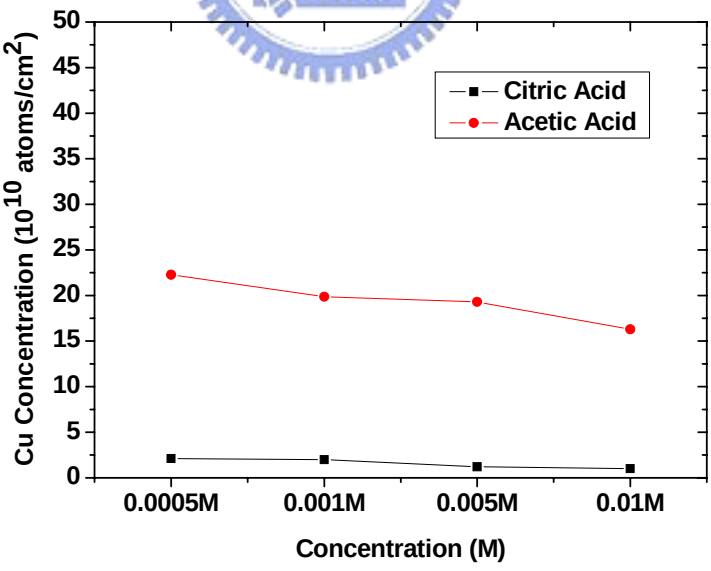

Figure.3-15 The cleaning efficiency as a function of concentration with cleaning cycle=40.

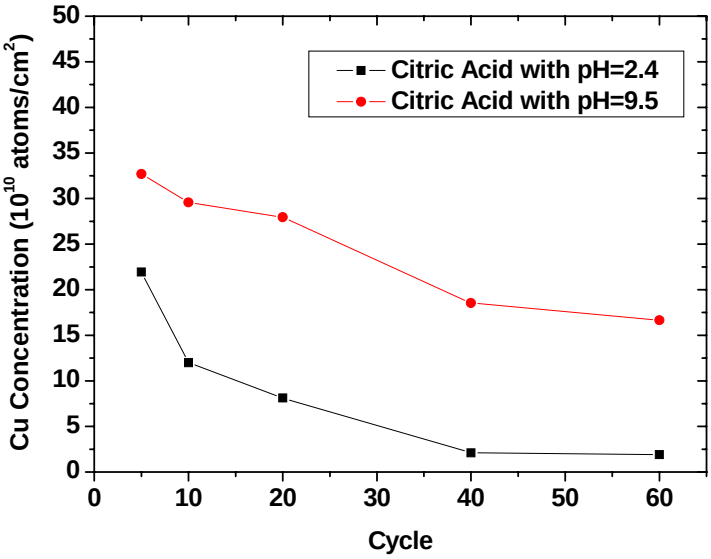

Figure.3-16 The cleaning efficiency as a function of citric acid cleaning cycle with concentration=5E^{-4}M.

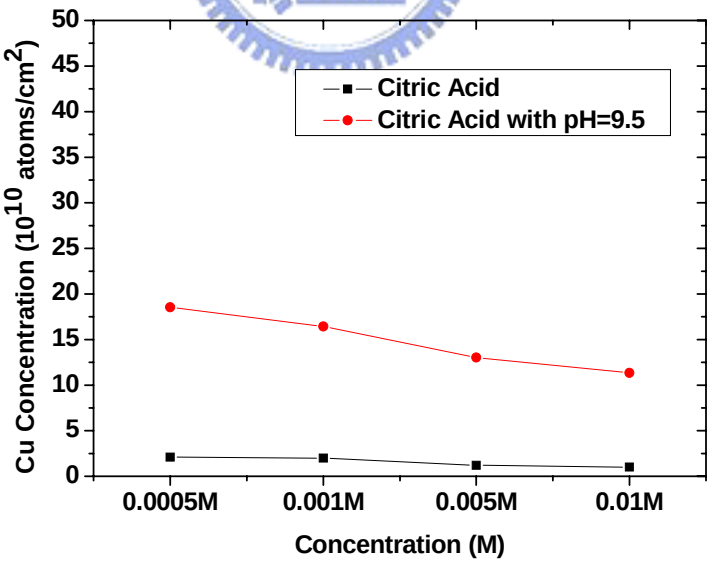

Figure.3-17 The cleaning efficiency as a function of citric acid concentration with cleaning cycle=40.

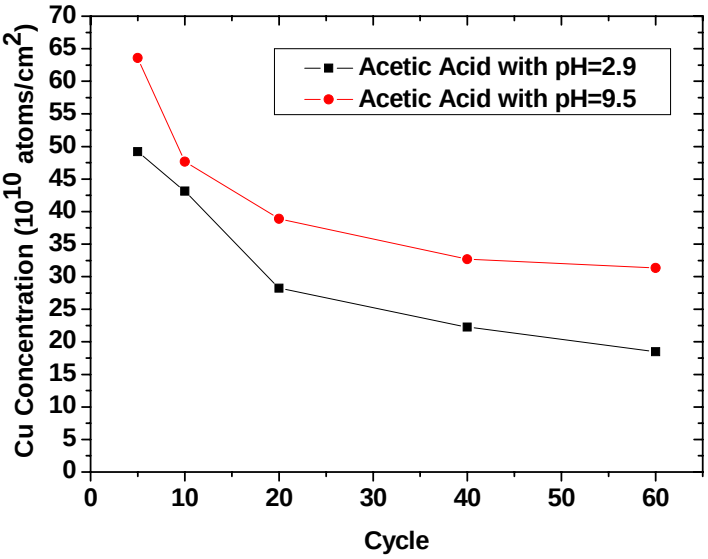

Figure.3-18 The cleaning efficiency as a function of acetic acid cleaning cycle with concentration=5E^{-4}M.

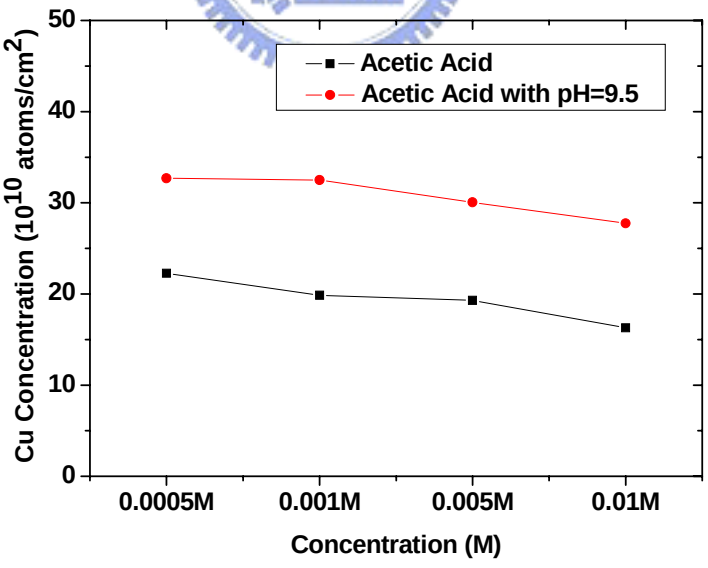

Figure.3-19 The cleaning efficiency as a function of acetic acid concentration with cleaning cycle=40.